Monthly Notices of the ROYAL ASTRONOMICAL SOCIETY

MNRAS **516,** 2653–2661 (2022) https://doi.org/10.1093/mnras/stac2394
Advance Access publication 2022 August 25

Hyperfine resolved rate coefficients of $HC^{17}O^+$ with H_2 ($j = 0$)

F. Tonolo [1,2★] F. Lique [3] M. Melosso [4] C. Puzzarini [2] and L. Bizzocchi [2★]

[1] *Scuola Normale Superiore, Piazza dei Cavalieri 7, I-56126 Pisa, Italy*
[2] *Dipartimento di Chimica 'Giacomo Ciamician', Università di Bologna, Via F. Selmi 2, I-40126 Bologna, Italy*
[3] *Institut de Physique de Rennes, Univ. Rennes, CNRS, IPR (Institut de Physique de Rennes) – UMR 6251, F-35000 Rennes, France*
[4] *Scuola Superiore Meridionale, Largo San Marcellino 10, I-80138 Naples, Italy*

Accepted 2022 August 13. Received 2022 July 13; in original form 2022 July 13

ABSTRACT

The formyl cation (HCO^+) is one of the most abundant ions in molecular clouds and plays a major role in the interstellar chemistry. For this reason, accurate collisional rate coefficients for the rotational excitation of HCO^+ and its isotopes due to the most abundant perturbing species in interstellar environments are crucial for non-local thermal equilibrium models and deserve special attention. In this work, we determined the first hyperfine resolved rate coefficients of $HC^{17}O^+$ in collision with H_2 ($j = 0$). Indeed, despite no scattering calculations on its collisional parameters have been performed so far, the $HC^{17}O^+$ isotope assumes a prominent role for astrophysical modelling applications. Computations are based on a new four dimensional (4D) potential energy surface obtained at the CCSD(T)-F12a/aug-cc-pVQZ level of theory. A test on the corresponding cross-section values pointed out that, to a good approximation, the influence of the coupling between rotational levels of H_2 can be ignored. For this reason, the H_2 collider has been treated as a spherical body and an average of the potential based on five orientations of H_2 has been employed for scattering calculations. State-to-state rate coefficients resolved for the $HC^{17}O^+$ hyperfine structure for temperature ranging from 5 to 100K have been computed using recoupling techniques. This study provides the first determination of $HC^{17}O^+$–H_2 inelastic rate coefficients directly computed from full quantum close-coupling equations, thus supporting the reliability of future radiative transfer modellings of $HC^{17}O^+$ in interstellar environments.

Key words: molecular data – molecular processes – scattering – ISM: abundances.

1 INTRODUCTION

When aiming at a deeper knowledge of the physical and chemical properties of star forming regions, the formyl cation (HCO^+) and its isotopic variants undoubtedly represent one of the most attracting systems for a number of reasons. HCO^+ is widespread and abundant through many evolutionary stages of the interstellar medium (ISM) and its formation path is straightforward and well understood (Herbst & Klemperer 1973). Due to its ionic nature, it plays a major role both in the interstellar chemistry and the dynamics of the interstellar gas. It also provides much information on the characteristics of the sources responsible for its heating and ionization (Guélin, Langer & Wilson 1982a; Jørgensen, Schöier & Van Dishoeck 2004). Moreover, its main destruction route occurs by dissociative recombination, making its abundance closely related to the electron density of the studied region (Wootten, Snell & Glassgold 1979).

Generally speaking, the capability of modelling the collisional excitation is critical to derive reliable molecular abundance from the emission spectra of interstellar clouds (Roueff & Lique 2013). This is particularly true for species that are abundant in the ISM, since their emission lines are often optically thick. To this aim, many efforts have been made in order to retrieve accurate state-to-state collisional rate coefficients for HCO^+ interacting with the He and H_2 (Massó & Wiesenfeld 2014; Yazidi, Ben Abdallah & Lique 2014; Tonolo et al. 2021), as well as for some of its isotopologues (see e.g. Pagani, Bourgoin & Lique 2012, Denis-Alpizar et al. 2020 and references therein).

However, in spite of several spectroscopic studies and astrophysical detections (see e.g. Guélin, Cernicharo & Linke 1982b; Plummer, Herbst & De Lucia 1983; Dore, Cazzoli & Caselli 2001), to the best of our knowledge, a thorough study of the collision physics of the $HC^{17}O^+ - H_2$ system has not been carried out yet. The rotational transitions of the ^{17}O-bearing variant exhibit hyperfine structure due to the splitting of its rotational energy levels by the electric quadrupole coupling of the ^{17}O ($I = 5/2$) nucleus. When properly treated, the hyperfine structure is a precious source of information as the observed intensities for the various hyperfine components provide a mean to constrain the optical depth. Given the above motivations, the availability of up-to-date collisional data of $HC^{17}O^+$ with the major astrophysical collision partners gains a substantial importance.

With the aim of filling this lack, we present here the first calculation of the hyperfine state-to-state rate coefficients for $HC^{17}O^+$ with H_2 ($j = 0$) system based on a new four dimensional (4D) interaction potential. The paper is structured as follows. In Section 2, the adopted computational procedure is described. In more detail, the approach employed to accurately describe the interaction potential between $HC^{17}O^+$ and H_2 is provided in Section 2.1. In Section 2.2,

★ E-mail: francesca.tonolo@sns.it (FT); luca.bizzocchi@unibo.it (LB)

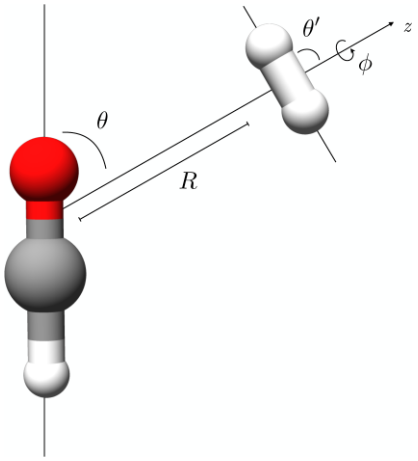

Figure 1. Jacobi internal coordinates of the HCO^+–H_2 collisional system.

the computation of the collisional cross sections are described (Section 2.2.1), and the collisional rate coefficients are reported and analysed (Section 2.2.2). Moreover, Section 3 assesses the impact given by isotopic substitution on the values of the computed rate coefficients. Finally, a comparison of the rate coefficients obtained with the almost exact recoupling approach and those derived from infinite order sudden (IOS) based approximation (Faure & Lique 2012) and statistical methods is provided in Section 4 with the aim of estimating the impact of such approximations on radiative transfer applications.

2 COMPUTATIONAL DETAILS

2.1 Potential energy surface

The first step in computing the scattering parameters of a collisional system is the determination of the corresponding potential energy surface (PES). Within the Born–Oppenheimer (BO) approximation, the interaction energy of the fragments does not depend on the chosen isotopologue for either the target or the collider species, the only difference is the shift of the Jacobi coordinates, used to describe the scattering due to the variation of the centre of mass. To investigate the $HC^{17}O^+$ and H_2 collisional system, we thus decided to study the PES involving the parent species ($HC^{16}O^+$). Such a choice allowed for a direct test of the accuracy of our methodology by comparison with previous calculations (Massó & Wiesenfeld (2014), Yazidi et al. (2014)). The effect of the isotopic substitution is then accounted for by shifting the centre of mass of the target in the PES before performing scattering calculations.

To describe the collisional system, a set of four Jacobi coordinates has been used (see Fig. 1 for a graphical representation), i.e. the R distance between the centre of mass of HCO^+ and that of H_2, the θ angle between the HCO^+ molecular axis and the R vector, and, finally, the θ' and ϕ angles that orient the H_2 molecule in the HCO^+–R plane and out of it, respectively. HCO^+ and H_2 were considered as rigid rotors since under non-reactive low-temperature conditions, all the vibrational channels are closed for all of the rotational channels taken into account. Furthermore, previous studies have shown that the rigid rotor approximation is accurate enough for low-temperature scattering applications, whenever collisional energies are lower than the bending frequency (Stoecklin et al. 2013). The geometry of HCO^+ was held fixed at its experimentally determined equilibrium structure (linear): $r_{CH} = 1.0920$ Å, and $r_{CO} = 1.1056$ Å (Dore et al. 2003). For H_2, we used the bond length $r_{HH} = 0.7667$ Å, which corresponds to the vibrationally averaged value of its ground state (Jankowski & Szalewicz 1998).

The interaction energies between HCO^+ and H_2 have been computed by employing an explicitly correlated method denoted by the -F12 suffix (Adler, Knizia & Werner 2007; Peterson, Adler & Werner 2008; Knizia, Adler & Werner 2009) based on the coupled cluster theory and accounting for the singles, doubles, and a perturbative treatment of triples excitations (CCSD(T), Raghavachari et al. 1989). This has been combined with a correlation consistent quadruple-ζ quality basis set, thus leading to the CCSD(T)-F12/aug-cc-pVQZ level of theory (Dunning 1989). This choice was supported by the demonstrated accuracy of explicitly correlated methods in describing long- and short-range multidimensional PESs (Lique, Kłos & Hochlaf 2010; Ajili et al. 2013). Moreover, the addition of diffuse functions in the basis set improves the description of the electronic behaviour for molecular systems involving non-covalent interactions (Kendall, Dunning & Harrison 1992; Lupi et al. 2021). All calculations were carried out with the MOLPRO suite of programs (Werner et al. 2012).

The interaction energy E_{int} has been computed as:

$$E_{int} = E_{AB} - (E_A + E_B), \tag{1}$$

where E_{AB} is the molecular complex energy, while E_A and E_B are the energies of the two fragments (here generally denoted as A and B). Each energy has also been corrected for the basis set superposition error (BSSE) by means of the counterpoise (CP) correction scheme. The CP correction is computed using the Boys & Bernardi (1970) scheme:

$$\Delta E_{CP} = \left(E_A^{AB} - E_A^A\right) + \left(E_B^{AB} - E_B^B\right), \tag{2}$$

where E_X^{AB} is the energy of the monomer calculated with the same basis set used for the cluster and E_X^X is the energy of the monomer computed with its own basis set (X = A, B).

We mapped the PES of the collisional system by selecting an irregular grid of 3375 points in the $\{R, \theta, \theta', \phi\}$ set of coordinates. We chose 25 values of the θ angle equally spaced from 0 to 180° and 27 R distances, which vary between 2.5 and 10 Å with a denser mesh in the proximity of the potential well. Finally, for each set of R and θ, five different orientations of H_2 with respect to HCO^+ (θ' and ϕ angles) have been selected. The use of such a limited subset of target-collider orientations is discussed more in detail in the following paragraphs.

To solve the close-coupling equations, a suitable angular expansion of the PES for each inter-molecular distance R is needed. For the HCO^+–H_2 collisional system, this expansion assumes the form of an interaction potential between two linear rigid rotors (Green 1975; Wernli et al. 2007a, b):

$$V(R, \theta, \theta', \phi) = \sum_{l_1 l_2 \mu} v_{l_1 l_2 \mu}(R) s_{l_1 l_2 \mu}(\theta, \theta', \phi), \tag{3}$$

where $v_{l_1 l_2 \mu}(R)$ are the radial coefficients and the l_1, l_2, and μ indices are associated with the rotational angular momenta of $HCO^+(j_1)$, $H_2(j_2)$, and with their vector sum, respectively. In equation (3), the centrosymmetric nature of H_2 forces the index l_2 to be even. The $s_{l_1 l_2 \mu}$ coefficients are defined as products of spherical harmonics ($Y_{l_i m}(\theta, \phi)$) and the Clebsch–Gordan vector-coupling coefficients (see Green 1975; Brown, Brown & Carrington 2003; Edmonds 2016

for further details):

$$s_{l_1 l_2 \mu}(\theta, \theta', \phi) = \left(\frac{2l_1+1}{4\pi}\right)^{1/2} \Bigg\{ \langle l_1 0 l_2 0 | l_1 l_2 \mu 0\rangle P_{l_1 0}(\theta) P_{l_2 0}(\theta') + \sum_m (-1)^m 2 \langle l_1 m l_2 - m | l_1 l_2 \mu 0\rangle \times P_{l_1 m}(\theta) P_{l_2 m}(\theta') \cos(m\phi) \Bigg\}, \quad (4)$$

where $P_{l_i m}(\theta) = Y_{l_i m}(\theta, \phi) e^{-i m \phi}$.

Previous studies (Faure et al. 2005; Wernli et al. 2006) have shown that the basis terms with $l_2 > 2$ in the expansion of the potential can be safely neglected in the description of the HCO^+–H_2 interaction. This significantly reduces the computational effort, since the only basis functions that describe the dependence of the potential on the relative orientations of H_2 are the Y_{00}, Y_{20}, Y_{21}, and Y_{22} spherical harmonics. At fixed R and θ values, the dependence of the potential on the orientation of H_2 is thus entirely described by the knowledge of only four orientations $\{\theta', \phi\}$ of H_2. Hence, the choice of five sets of $\{\theta', \phi\}$ angles is not only sufficient to describe the dependence of the potential on them, but also allows for an over-determined system to test the accuracy of the l_2 truncation. The five orientations chosen to describe the relative rotations of H_2 with respect to the target molecule are:

$$x \rightarrow \left(\theta' = \frac{\pi}{2}, \phi = 0\right); \quad (5a)$$

$$y \rightarrow \left(\theta' = \frac{\pi}{2}, \phi = \frac{\pi}{2}\right); \quad (5b)$$

$$z \rightarrow (\theta' = 0, \phi = 0); \quad (5c)$$

$$a \rightarrow \left(\theta' = \arccos\left(\frac{1}{\sqrt{3}}\right), \phi = \frac{\pi}{4}\right); \quad (5d)$$

$$b \rightarrow \left(\theta' = \pi - \arccos\left(\frac{1}{\sqrt{3}}\right), \phi = \frac{\pi}{4}\right). \quad (5e)$$

They are the same used by Wernli et al. (2007a) for the HC_3N–H_2 system.

We performed a two dimensional (2D) fit of the potential for each of the five sets of $\{\theta', \phi\}$ orientations, following the same procedure described by Tonolo et al. (2021) for the interacting HCO^+–He system. The *ab initio* values and those obtained from the fitted radial coefficients of equation (3) differ by less than 1.5 per cent across the entire grid. Fig. 2 illustrates the topology of the potential obtained for each orientation of H_2: only minor anisotropy of the potential with respect to the orientation of H_2 is apparent, thus validating the choice to exclude the basis terms with $l_2 > 2$ in the angular expansion of the PES. Each 2D cut of the potential also exhibits a minimum for $\theta \sim 180°$, wherein the hydrogen molecule approaches the hydrogen side of HCO^+. In accordance with the findings of the benchmark study of Massó & Wiesenfeld (2014) on different levels of theory, the potential well has its maximum depth when the H_2 fragment is perpendicularly oriented with respect to the HCO^+ plane ($\theta = \pi$, $\phi = \pi/2$) and $R \sim 3.44$ Å.

Having assessed the correct behaviour of the potential for each orientation of H_2, the analytical dependence over $\{\theta', \phi\}$ was then introduced via the following equation (Wernli et al. 2006):

$$V(R, \theta_1, \theta', \phi') = V_{\rm av}(R, \theta) + \frac{1}{2}[V(R, \theta, z) - V_{\rm av}(R, \theta)](3\cos^2\theta' - 1) + \frac{3}{2}[V(R, \theta, a) - V(R, \theta, b)] \sin\theta' \cos\theta' \cos\phi' + \frac{1}{2}[V(R, \theta, x) - V(R, \theta, y)] \sin^2\theta' \cos(2\phi'), \quad (6)$$

where x, y, z, a, b correspond to the coordinates specified in equation (5) and

$$V_{\rm av}(R, \theta) = \frac{1}{7}[2(V(R, \theta, a) + V(R, \theta, b)) + (V(R, \theta, x) + V(R, \theta, y) + V(R, \theta, z))]. \quad (7)$$

This allowed us to fully include the rotational structure of H_2 in the scattering calculations, thus also incorporating the couplings with the H_2 ($j > 0$) rotational states. However, a dedicate test (see next section for details) showed that the effects of such coupling on the rate coefficients is negligible, as already found for the HCO^+–H_2 collisional system (Massó & Wiesenfeld 2014). Only the leading term $l_2 = \mu = 0$ needs thus to be retained in the expansion of the interaction potential expressed equation (3).

This corresponds to further simplify the expansion of the potential to the interaction of a rigid linear body with a sphere (Lique et al. 2008; Dumouchel, Kłos & Lique 2011):

$$V_{\rm av}(R, \theta) = \sum_{l_1} v_{l_1}(R) P_{l_1}(\cos(\theta)), \quad (8)$$

where the quantity $V_{\rm av}(R, \theta)$ is the potential averaged over the angular motion of H_2, already defined in equation (7). This formulation of the potential reduces the description of the PES to a two-dimensional problem, thus significantly simplifying the computational effort of scattering calculations. A contour plot of the potential derived from the fit is shown in Fig. 3.

A spherical average of the HCO^+–H_2 potential was also previously performed by Yazidi et al. (2014) but, unlike us, they accounted for only three orientations of H_2. Comparing the topology of the two PESs, the agreement is good. Both potentials exhibit a strong anisotropy with respect to the θ angle and present a global minimum at $R = 3.6$ Å and $\theta = 180°$. Since we have adopted an higher level of theory, the present PES represents – to date – the most accurate description of a spherical potential on the targeted system.

2.2 Scattering calculations

2.2.1 *Inelastic cross sections*

With the aim of computing the rate coefficients of the $HC^{17}O^+$–H_2 collisional system, the most reliable approach is to perform full quantum close-coupling (CC) calculations on the interaction potential shifted for the $^{16}O \rightarrow {}^{17}O$ isotope substitution. This isotopic substitution introduces a new feature due to the ^{17}O nuclear spin (angular momentum $I = 5/2$), which couples with the molecular rotational angular momentum **j** through electric quadrupole interaction. The total angular momentum of the molecule **F** is thus defined by the $\mathbf{j} + \mathbf{I}$ vector sum. This leads to the splitting of each rotational level into various F sublevels with F varying between $|I - j|$ and $I + j$. Since the energy splittings due to the interaction structure are much smaller than those between rotational levels, a common approximation is to ignore, at a first stage, such coupling contribution from the molecular

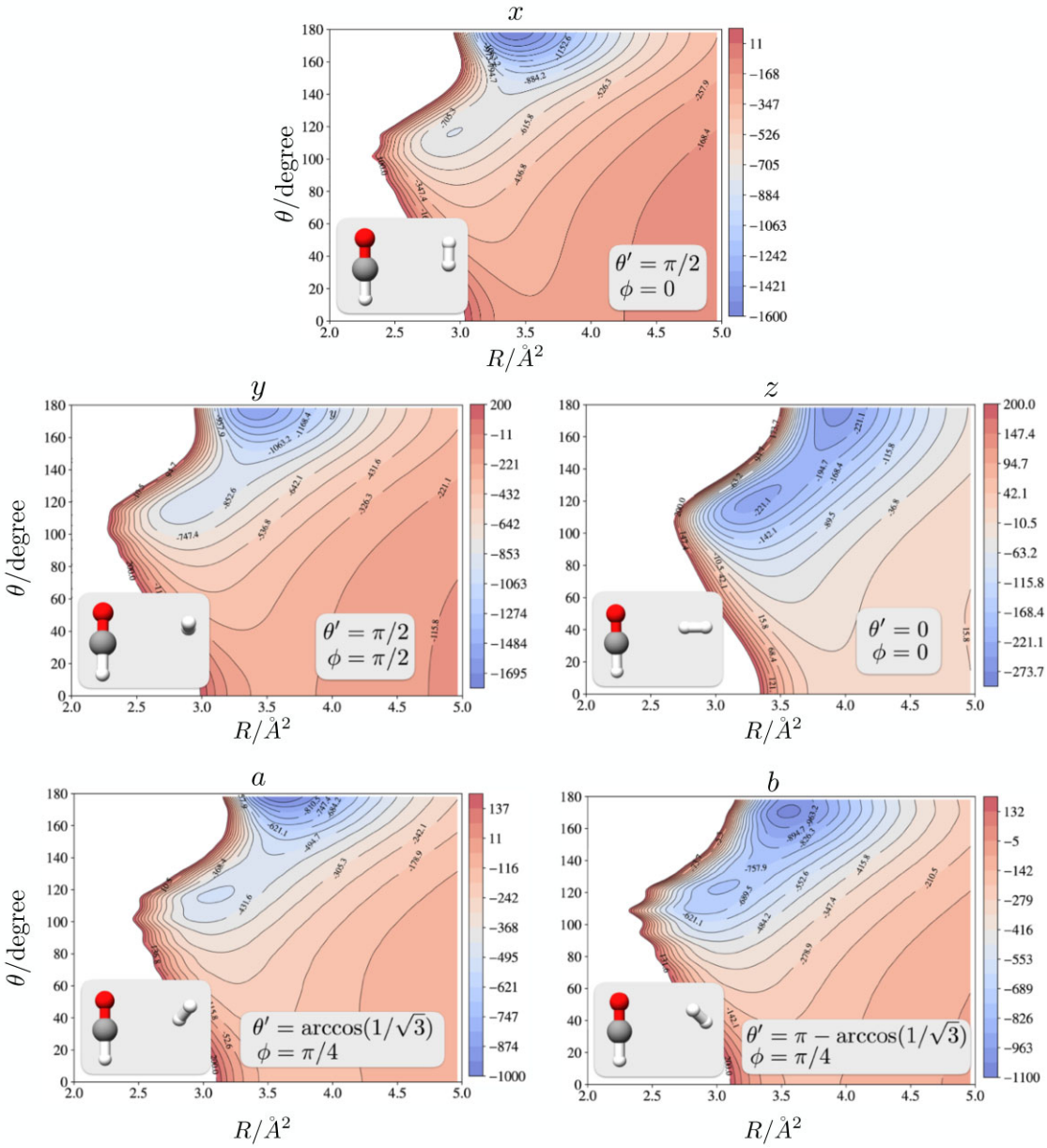

Figure 2. Contour plots of the HCO^+–H_2 interaction PES for five different orientations of H_2 with respect to HCO^+ as a function of R and θ. Energies are in cm^{-1}.

Hamiltonian and to subsequently decouple the spin wave-functions from the rotational ones using the recoupling method described by Alexander & Dagdigian (1985). In detail, the inelastic cross-sections associated with a $jF \rightarrow j'F'$ transition are obtained from the rotational scattering matrix elements $S^J(jl; j'l')$ (nuclear-spin free) derived from the close-coupling (CC) calculations:

$$T^J(jl; j'l') = 1 - S^J(jl; j'l'). \tag{9}$$

$T^J(jl; j'l')$ are the T-matrix elements, which are linked to the opacities tensor $P^K(j \rightarrow j')$ via

$$P^K(j \rightarrow j') = \frac{1}{2K+1} \sum_{ll'} |T^K(jl; j'l')|^2, \tag{10}$$

where

$$T^K(jl; j'l') = (-1)^{-j-l'}(2K+1) \sum_J (-1)^J (2J+1) \times \begin{Bmatrix} l' & j' & J \\ j & l & K \end{Bmatrix} T^J(jl; j'l'). \tag{11}$$

From the opacity tensor elements $P^K(j \rightarrow j')$, the recoupled inelastic cross sections $\left(\sigma^{\mathrm{REC}}_{jF \rightarrow j'F'}\right)$ are obtained as:

$$\sigma^{\mathrm{REC}}_{jF \rightarrow j'F'} = \frac{\pi}{k^2_{jF}} (2F'+1) \sum_K \begin{Bmatrix} j & j' & K \\ F' & F & I \end{Bmatrix}^2 P^K(j \rightarrow j'). \tag{12}$$

This method is approximate, but almost exact and therefore is commonly considered as a 'reference' approach (Faure & Lique (2012)).

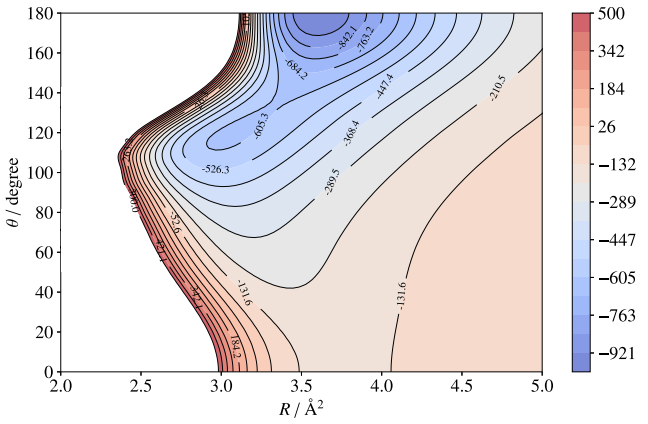

Figure 3. Contour plot of the HCO^+–H_2 interaction PES for the averaged potential V_{av} (equation 7) as a function of R and θ. Energies are in cm^{-1}.

Table 1. Computed cross sections at $E = 50\,cm^{-1}$ for $HC^{17}O^+ - H_2(j = 0)$ collisions obtained from the 2D spherically averaged potential and the full 4D potential which includes the coupling with $j = 2$ rotational level of H_2.

$j \rightarrow j'$	Cross sections / Å^2		Per cent error
	4D	2D	
$1 \rightarrow 0$	58.14	53.41	− 8.86
$2 \rightarrow 0$	52.59	50.31	− 4.54
$3 \rightarrow 0$	46.12	44.00	− 4.84
$4 \rightarrow 0$	27.26	30.28	9.98
$5 \rightarrow 0$	16.81	15.74	− 6.80
$2 \rightarrow 1$	59.78	60.87	1.80
$3 \rightarrow 1$	48.43	53.18	8.92
$4 \rightarrow 1$	36.70	35.19	− 4.30
$5 \rightarrow 1$	17.09	18.77	8.93
$3 \rightarrow 2$	55.24	52.95	− 4.32
$4 \rightarrow 2$	45.75	41.75	− 9.56
$5 \rightarrow 2$	20.39	21.02	3.01
$4 \rightarrow 3$	56.79	51.02	− 11.31
$5 \rightarrow 3$	24.43	23.19	− 5.35
$5 \rightarrow 4$	40.04	35.63	− 12.39
Average absolute per cent error			6.99

As mentioned in the previous section, a preliminary test on the influence of the coupling between $j = 0$ and $j > 0$ rotational states of H_2 was performed in order to evaluate the reliability of the 2D potential spherically averaged over the H_2 orientations. We thus compared the values of the $j(H_2) = 0$ partial cross sections computed for a single value of the total energy ($50\,cm^{-1}$) using the global 4D (equation 3), thus accounting for the $j = 0$, 2 coupling, and the reduced 2D (equation 7) potentials. The results are shown in Table 1: the pairs of values exhibit a mean average percentage error of ∼7 per cent and a maximum discrepancy of 12.4 per cent. This validated the results given by the spherical average potential approximation, which was then applied to the entire energy grid. In the following, the H_2 projectile is thus considered as a structureless species, behaving as a rotating sphere (*para*-H_2 with $j = 0$).

All scattering calculations have been carried out by employing the MOLSCAT program (Hutson & Green 1994) at values of the kinetic energy ranging from 2 to $500\,cm^{-1}$ with narrower steps at low energies ($0.2\,cm^{-1}$), which gradually increase as the energy rises. The adopted propagator is a hybrid one between the Manolopoulos diabatic modified log-derivative propagator and the Alexander–Manolopoulos–Airy propagator (LDMD/AIRY) (Alexander 1984; Manolopoulos 1986; Alexander & Manolopoulos 1987). This provides the correct compromise between computational efficiency and accuracy in the description of the potential, since it differently deals with the short- and long-range propagation according to the potential requirements, and thus using narrower propagation steps when the energy gradient is higher. The integration range was set from 2.5 Å to a long-range limit value purposely chosen to ensure convergence of the inelastic cross sections for the considered energy range. The same scheme has been applied to the rotational basis cut-off of $HC^{17}O^+$, which has been optimized for each energy range from a minimum value of $j = 25$ at $2\,cm^{-1}$ up to a maximum of $j = 31$ at the highest energies (above $300\,cm^{-1}$). The maximum value of the total angular momentum $\mathbf{J} = \mathbf{j} + \mathbf{l}$ has been chosen as the one that allowed for the convergence of the inelastic cross sections within 0.005 Å, reaching a maximum value of $J = 118$ at $500\,cm^{-1}$. The reduced mass of the collisional system is set to 1.8709 u and the rotational energies have been computed from the experimental ground-state spectroscopic constants (Dore et al. 2001): $B_0\,(HC^{17}O^+) = 43528.92$ MHz, $D_0\,(HC^{17}O^+) = 78.96$ kHz. The energies of the hyperfine levels of $HC^{17}O^+$ required for the recoupling calculation have been taken from Bizzocchi (2022).

Table 2. Hyperfine resolved (de-)excitation rate coefficients of the two lowest rotational levels for $T = 10$, 30, and 50K.

$j, F \rightarrow j', F'$	$k_{jF \rightarrow j'F'}/10^{-10}cm^3\,s^{-1}$		
	10K	30K	50K
$1, 1.5 \rightarrow 0, 2.5$	1.85	1.54	1.45
$0, 2.5 \rightarrow 1, 1.5$	0.81	0.89	0.89
$1, 2.5 \rightarrow 0, 2.5$	1.85	1.54	1.45
$0, 2.5 \rightarrow 1, 2.5$	1.22	1.34	1.34
$1, 2.5 \rightarrow 1, 1.5$	1.09	0.75	0.60
$1, 1.5 \rightarrow 1, 2.5$	1.63	1.13	0.91
$1, 2.5 \rightarrow 1, 3.5$	2.45	1.73	1.41
$1, 3.5 \rightarrow 1, 2.5$	1.83	1.29	1.06
$1, 3.5 \rightarrow 0, 2.5$	1.85	1.54	1.45
$0, 2.5 \rightarrow 1, 3.5$	1.63	1.78	1.78
$1, 3.5 \rightarrow 1, 1.5$	1.37	0.98	0.81
$1, 1.5 \rightarrow 1, 3.5$	2.73	1.95	1.62

2.2.2 *Hyperfine-resolved rate coefficients*

Having computed the inelastic cross sections $\sigma^{REC}_{jF \rightarrow j'F'}$, the corresponding rate coefficients are straightforwardly derived at a given temperature T by averaging over collision energy (E_c):

$$k_{jF \rightarrow j'F'}(T) = \left(\frac{8}{\pi \mu k_B^3 T^3}\right)^{1/2} \int_0^\infty \sigma^{REC}_{jF \rightarrow j'F'}\, E_c\, e^{-E_c/k_BT}\, dE_c. \quad (13)$$

We have obtained hyperfine resolved (de-)excitation rate coefficients for the lowest six rotational levels in the 5–100K range. The complete set of them will be made available through the LAMDA (Schöier et al. 2005; van der Tak et al. 2020) and BASECOL (Dubernet et al. 2013) data bases. A list of the rate coefficients involving the first two rotational levels at 10, 30, and 50K is presented in Table 2, while Figs 4 and 5 depict the variation of some de-excitation rate coefficients with temperature. In Fig. 4, the trend of the inelastic rate coefficients involving the same final hyperfine state is provided, whereas Fig. 5 shows the quasi-elastic rate coefficients into the $j = 1$ and $j = 2$ rotational levels. From both, a propensity towards the transitions involving the final hyperfine level (F') with the highest multiplicity clearly stands out. In addition, inelastic rate coefficients

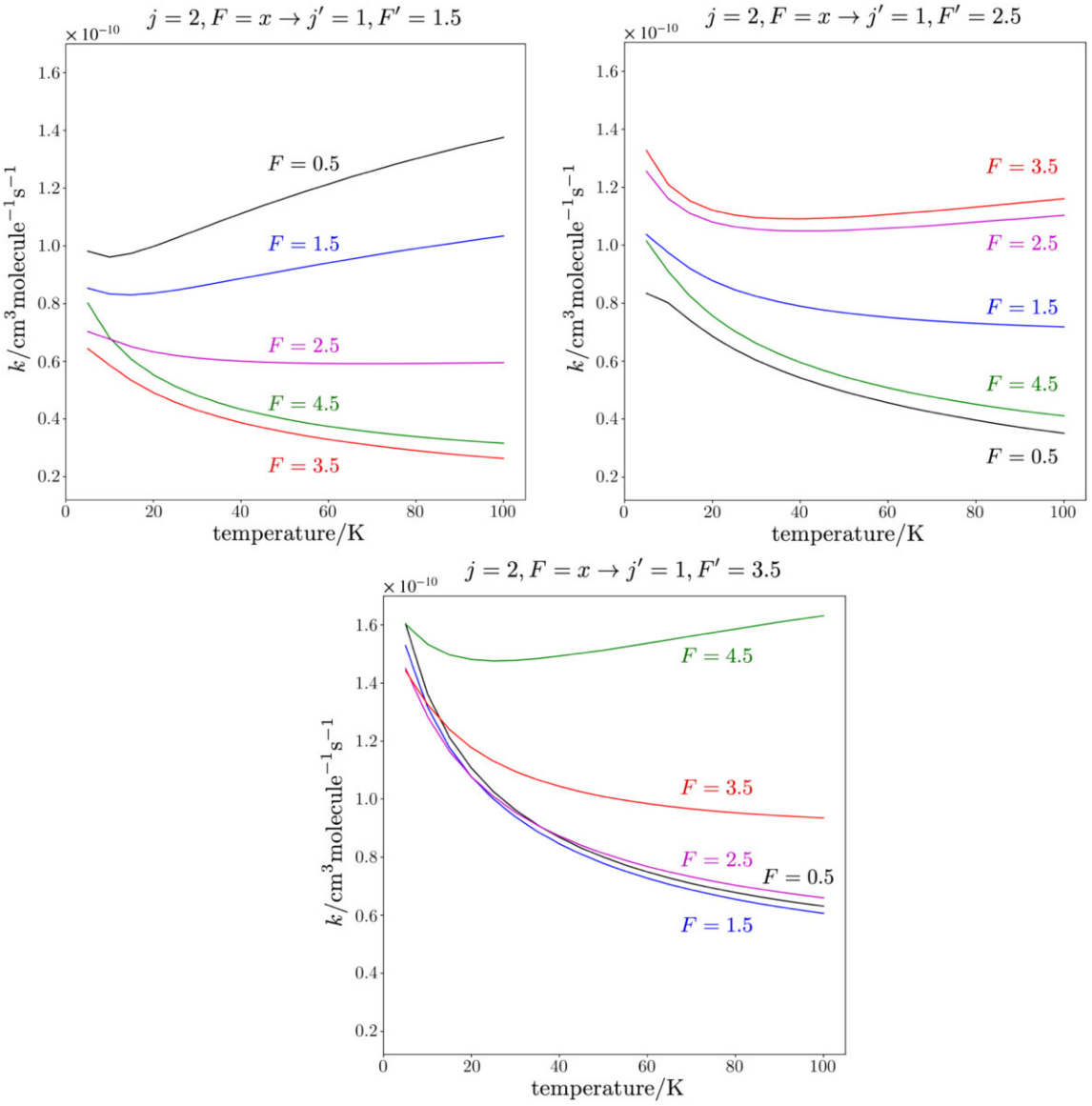

Figure 4. Temperature variation of the hyperfine resolved $HC^{17}O^+$–H_2 rate coefficients for some transitions involving the same final hyperfine state.

exhibit a propensity toward transitions involving $\Delta F = \Delta j$ when $F' \geq I$ and $-\Delta F = \Delta j$ when $F' < I$.

3 ISOTOPIC EFFECT

For astrophysical purposes, it is often assumed that collisional rate coefficients of a main isotopologue can be used to estimate rate coefficients for other isotopic variants. To test the reliability of this approximation for the $^{16}O \rightarrow {}^{17}O$ isotope substitution, we compared the values of the cross-section computed at $E = 50\,\mathrm{cm}^{-1}$ for the HCO^+ and $HC^{17}O^+$ target species. These two scattering system differ by the position of the centre of mass, the rotational constants of the target and the reduced masses. The results, reported in Table 3, exhibited significant discrepancies with an average percentage difference of more than 20 per cent. Noteworthy, the variation between the cross sections of HCO^+ and $HC^{17}O^+$ seems not to follow any kind of predictable pattern. Therefore, we expect that the use of scaled rate coefficients derived from the parent species would lead to unreliable results in radiative transfer modelling of astrophysical $HC^{17}O^+$ emission.

4 COMPARISON WITH APPROXIMATED RATE COEFFICIENTS

The recoupling approach used in the present work to compute hyperfine-resolved rate coefficients is almost exact but requires to store the $S^J(jl; j'l')$ elements and to compute the opacity tensor between the rotational levels of $HC^{17}O^+$, which implies a significant computational effort. To avoid such a demanding step, various approximate methodologies are frequently employed. A simple approach that is widely used for astrophysical applications (see Guilloteau & Baudry 1981; Keto & Rybicki 2010) is the statistical method called M_j-randomizing limit or proportional approach (RAN, Alexander & Dagdigian 1985). This method assumes a statistical reorientation of the quantum number F' after the collision, thus neglecting any dependence on the initial conditions of the system. This allows to express the $jF \rightarrow j'F'$ hyperfine-resolved rate coefficients

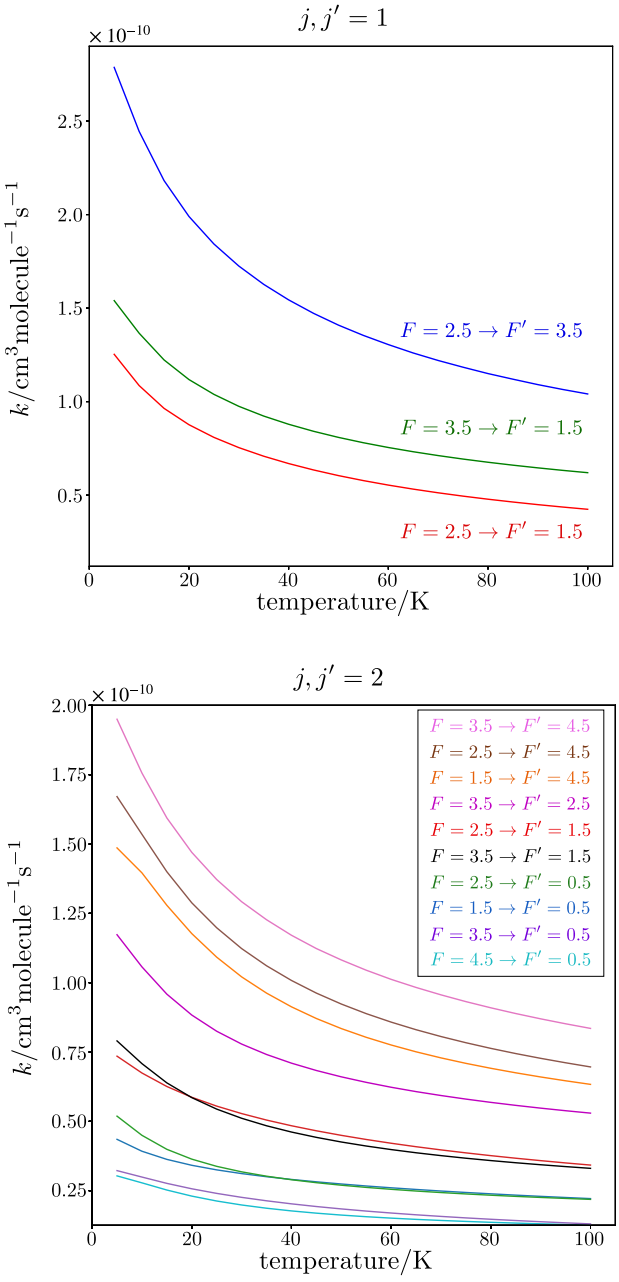

Figure 5. Temperature variation of the hyperfine resolved $HC^{17}O$–H_2 quasi-elastic rate coefficients involving the $j = 1, 2$ rotational levels.

from the corresponding pure rotational one $j \rightarrow j'$ through

$$k_{jF \rightarrow j'F'}(T) = \frac{(2F'+1)}{(2j'+1)(2I+1)} k_{j \rightarrow j}(T). \quad (14)$$

A way to account for the collision propensities given by the Wigner coefficients of equation (12) is provided by the Neufeld & Green (1994) approximation (NG). This approach is based on the IOS method which ignores the rotational energy spacing with respect to the collision energy, and derives the rate coefficients between hyperfine structure levels from the rotational excitation rate involving the fundamental $j = 0$ state (for more in-depth description, see Faure & Lique 2012 and references therein).

To assess the impact of these approximations on a typical non-LTE radiative transfer modelling, we have compared the hyperfine rate coefficients obtained with the full quantum CC approach plus recoupling with those derived from the corresponding rotational collision data employing the NG and RAN approximations. The results at 10K and 100K are shown in Fig. 6. At low temperature, the collisions are slow and typically go through the formation of a long lifetime $HC^{17}O^+$–H_2 complex in the potential well. When the complex dissociates, the level population evolves to a randomized distribution according to the statistical weights of the final states (F'). For this reason, the RAN approximation performs better at low temperatures at which statistical effects have a major impact on the rate coefficients. Conversely, the NG method is less accurate in describing the rate coefficients at low temperatures, where the assumption of neglecting rotational energy spacing compared to the collision energy is no longer valid. On the other hand, at higher temperatures, the influence of the propensity rules given by the Wigner coefficients becomes increasingly prominent, thus making the NG approach a better approximation.

Table 3. Computed cross-sections at $E = 50\,\mathrm{cm^{-1}}$ for the $HC^{17}O^+$/HCO^+ and $H_2(j = 0)$ collisions.

$j \rightarrow j'$	Cross sections / Å^2		Per cent error
	$HC^{17}O^+$	HCO^+	
$1 \rightarrow 0$	53.41	64.96	21.62
$2 \rightarrow 0$	50.31	55.34	10.00
$3 \rightarrow 0$	44.00	47.18	7.24
$4 \rightarrow 0$	30.28	41.16	35.90
$5 \rightarrow 0$	15.74	20.49	30.20
$2 \rightarrow 1$	60.87	60.25	– 1.03
$3 \rightarrow 1$	53.18	49.24	– 7.40
$4 \rightarrow 1$	35.19	40.20	14.22
$5 \rightarrow 1$	18.77	18.88	0.59
$3 \rightarrow 2$	52.95	64.27	21.39
$4 \rightarrow 2$	41.75	51.14	22.47
$5 \rightarrow 2$	21.02	23.86	13.47
$4 \rightarrow 3$	51.02	61.93	21.38
$5 \rightarrow 3$	23.19	37.58	62.02
$5 \rightarrow 4$	35.63	47.33	32.85
Average absolute per cent error			20.12

5 CONCLUSIONS

In this work, we presented the first computed rate coefficients for the hyperfine (de-)excitation of $HC^{17}O^+$ by collisions with H_2 ($j = 0$), the most abundant collisional partner in cold molecular clouds. First, we characterized the involved PES by exploiting the accuracy of explicitly correlated coupled-cluster calculations, employing the CCSD(T)-F12a/aug-cc-pVQZ level of theory. The interaction energy was averaged over five H_2 orientations and then fitted by means of the procedure described by Werner et al. (1989). Before performing scattering calculations, the effects due to the coupling between the different rotational states of H_2 ($j = 0, 2$) on the inelastic cross sections have been assessed. This permitted us to neglect, in a good approximation, the influence of $j(H_2) > 0$, thus allowing to perform spherical average of the potential with respect to the orientations of H_2. Finally, state-to-state rate coefficients between the six lowest rotational levels have been computed using recoupling techniques for temperatures ranging from 5 to 100K.

The importance of these data is highlighted by the significant difference between the values of the collision cross sections computed for HCO^+ and $HC^{17}O^+$. As a matter of facts, retrieving the

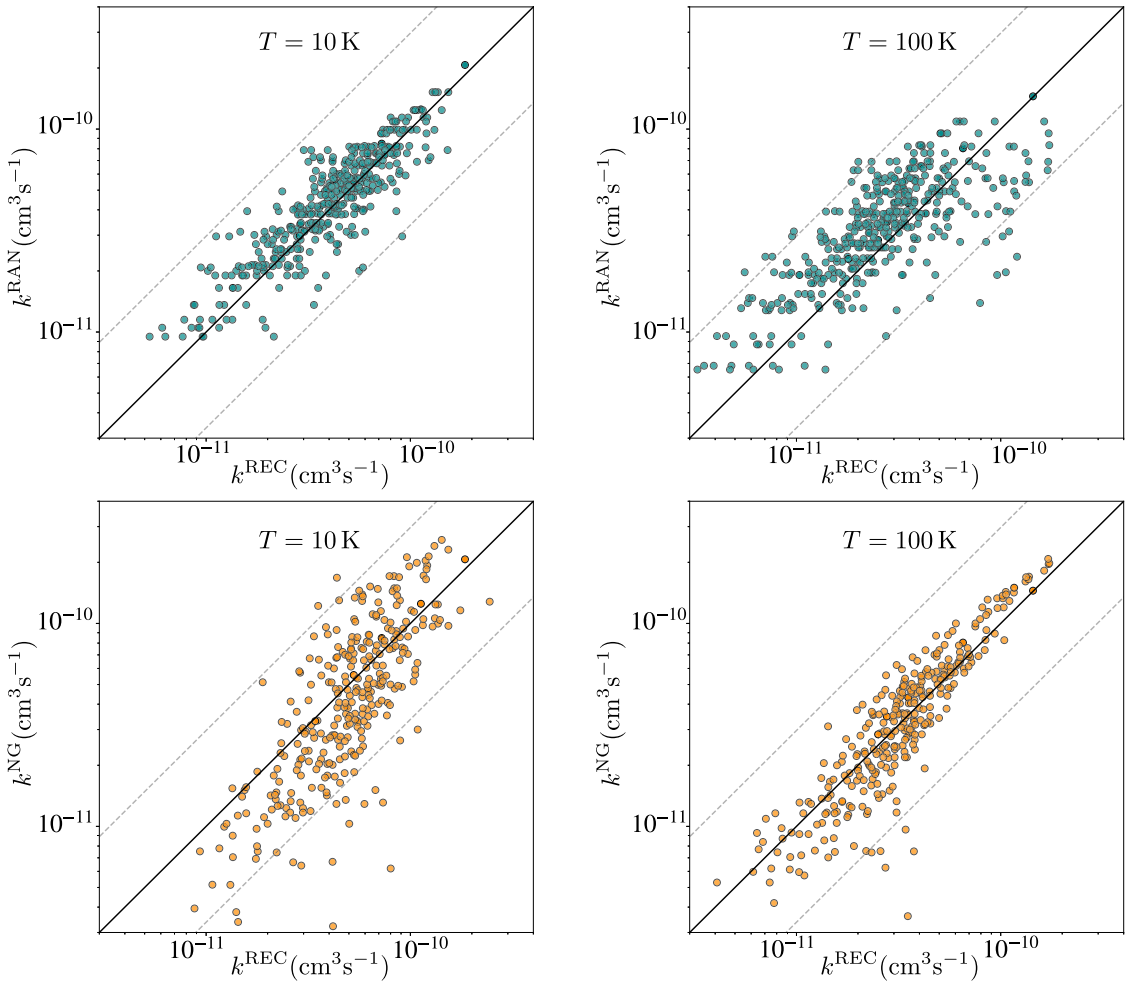

Figure 6. Comparison between $HC^{17}O^+$–H_2 recoupling hyperfine rate coefficients and those obtained using the RAN (top panels) and NG (bottom panels) approximations at 10K (left-hand panels) and 100K (right-hand panels). In each panel, the dashed lines delimit the region where the rate coefficients differ by less than a factor of three.

collisional rate coefficients of $HC^{17}O^+$ and H_2 by simply scaling the ones of the HCO^+–H_2 system does not represent a reliable approach. A similar behaviour is also expected for the $HC^{18}O^+$ isotopologue, which features an even more pronounced shift of the centre of mass with respect to the parent species. Furthermore, the comparison with commonly adopted approaches, such as RAN and NG approximations, indicates that the recoupling approach represents the most reliable methodology to compute hyperfine resolved inelastic rate coefficients for astrophysically interesting systems.

ACKNOWLEDGEMENTS

This study was supported by MUR (PRIN Grant Number 202082CE3T) and University of Bologna (RFO funds). The SMART@SNS Laboratory (http://smart.sns.it) is acknowledged for providing high-performance computing facilities. We also acknowledge financial support from the European Research Council (Consolidator Grant COLLEXISM, Grant Agreement No. 811363). F. Lique acknowledges financial support from the Institut Universitaire de France and the Programme National 'Physique et Chimie du Milieu Interstellaire' (PCMI) of INSU,CNRS with INC/INP cofunded by CEA and CNES.

DATA AVAILABILITY

The data underlying this article will be made available through the LAMDA (Schöier et al. 2005; van der Tak et al. 2020) and BASECOL (Dubernet et al. 2013) data bases. They are also available on request.

REFERENCES

Adler T. B., Knizia G., Werner H.-J., 2007, J. Chem. Phys., 127, 221106
Ajili Y., Hammami K., Jaidane N. E., Lanza M., Kalugina Y. N., Lique F., Hochlaf M., 2013, Phys. Chem. Chem. Phys., 15, 10062
Alexander M. H., 1984, J. Chem. Phys., 81, 4510
Alexander M. H., Dagdigian P. J., 1985, J. Chem. Phys., 83, 2191
Alexander M. H., Manolopoulos D. E., 1987, J. Chem. Phys., 86, 2044
Bizzocchi L., 2022, in prep
Boys S. F., Bernardi F., 1970, Mol. Phys., 19, 553
Brown J. M., Brown J. M., Carrington A., 2003, Rotational Spectroscopy of Diatomic Molecules. Cambridge Univ. Press, Cambridge
Denis-Alpizar O., Stoecklin T., Dutrey A., Guilloteau S., 2020, MNRAS, 497, 4276
Dore L., Cazzoli G., Caselli P., 2001, A&A, 368, 712
Dore L., Beninati S., Puzzarini C., Cazzoli G., 2003, J. Chem. Phys., 118, 7857
Dubernet M.-L. et al., 2013, A&A, 553, A50
Dumouchel F., Kłos J., Lique F., 2011, Phys. Chem. Chem. Phys., 13, 8204

Dunning T. H. Jr, 1989, J. Chem. Phys., 90, 1007
Edmonds A. R., 2016, Angular Momentum in Quantum Mechanics. Princeton Univ. Press, Princeton
Faure A., Lique F., 2012, MNRAS, 425, 740
Faure A., Wiesenfeld L., Wernli M., Valiron P., 2005, J. Chem. Phys., 123, 104309
Green S., 1975, J. Chem. Phys., 62, 2271
Guélin M., Langer W., Wilson R., 1982a, A&A, 107, 107
Guélin M., Cernicharo J., Linke R., 1982b, ApJ, 263, L89
Guilloteau S., Baudry A., 1981, A&A, 97, 213
Herbst E., Klemperer W., 1973, ApJ, 185, 505
Hutson J. M., Green S., 1994, MOLSCAT version 14, distributed by Collaborative Computational Project No. 6. Engineering and Physical Sciences Research Council, UK
Jankowski P., Szalewicz K., 1998, J. Chem. Phys., 108, 3554
Jørgensen J., Schöier F., Van Dishoeck E., 2004, A&A, 416, 603
Kendall R. A., Dunning T. H. Jr, Harrison R. J., 1992, J. Chem. Phys., 96, 6796
Keto E., Rybicki G., 2010, ApJ, 716, 1315
Knizia G., Adler T. B., Werner H.-J., 2009, J. Chem. Phys., 130, 054104
Lique F., Toboła R., Kłos J., Feautrier N., Spielfiedel A., Vincent L., Chałasiński G., Alexander M., 2008, A&A, 478, 567
Lique F., Kłos J., Hochlaf M., 2010, Phys. Chem. Chem. Phys., 12, 15672
Lupi J., Alessandrini S., Puzzarini C., Barone V., 2021, J. Chem. Theor. Comput., 17, 6974
Manolopoulos D., 1986, J. Chem. Phys., 85, 6425
Massó H., Wiesenfeld L., 2014, J. Chem. Phys., 141, 184301
Neufeld D. A., Green S., 1994, ApJ, 432, 158
Pagani L., Bourgoin A., Lique F., 2012, A&A, 548, L4
Peterson K. A., Adler T. B., Werner H.-J., 2008, J. Chem. Phys., 128, 084102
Plummer G., Herbst E., De Lucia F., 1983, ApJ, 270, L99
Raghavachari K., Trucks G. W., Pople J. A., Head-Gordon M., 1989, Chem. Phys. Lett., 157, 479
Roueff E., Lique F., 2013, Chem. Rev., 113, 8906
Schöier F. L., van der Tak F. F. S., van Dishoeck E. F., Black J. H., 2005, A&A, 432, 369
Stoecklin T., Denis-Alpizar O., Halvick P., Dubernet M.-L., 2013, J. Chem. Phys., 139, 034304
Tonolo F., Bizzocchi L., Melosso M., Lique F., Dore L., Barone V., Puzzarini C., 2021, J. Chem. Phys., 155, 234306
van der Tak F. F., Lique F., Faure A., Black J. H., van Dishoeck E. F., 2020, Atoms, 8, 15
Werner H. J., Knowles P. J., Knizia G., Manby F. R., Schütz M., 2012, WIREs Comput. Mol. Sci., 2, 242
Werner H.-J., Follmeg B., Alexander M. H., Lemoine D., 1989, J. Chem. Phys., 91, 5425
Wernli M., Valiron P., Faure A., Wiesenfeld L., Jankowski P., Szalewicz K., 2006, A&A, 446, 367
Wernli M., Wiesenfeld L., Faure A., Valiron P., 2007a, A&A, 464, 1147
Wernli M., Wiesenfeld L., Faure A., Valiron P., 2007b, A&A, 475, 391
Wootten A., Snell R., Glassgold A., 1979, ApJ, 234, 876
Yazidi O., Ben Abdallah D., Lique F., 2014, MNRAS, 441, 664

This paper has been typeset from a TEX/LATEX file prepared by the author.